JACS
JOURNAL OF THE AMERICAN CHEMICAL SOCIETY

Article

pubs.acs.org/JACS

Nitrile Probes of Electric Field Agree with Independently Measured Fields in Green Fluorescent Protein Even in the Presence of Hydrogen Bonding

Joshua D. Slocum and Lauren J. Webb*

Department of Chemistry, Center for Nano and Molecular Science and Technology, and Institute for Cell and Molecular Biology, The University of Texas at Austin, 105 E 24th Street STOP A5300, Austin, Texas 78712-1224, United States

Supporting Information

ABSTRACT: There is growing interest in using the nitrile vibrational oscillation as a site-specific probe of local environment to study dynamics, folding, and electrostatics in biological molecules such as proteins. Nitrile probes have been used extensively as reporters of electric field using vibrational Stark effect spectroscopy. However, the analysis of frequencies in terms of electric fields is potentially complicated by the large ground state dipole moment of the nitrile, which may irrevocably perturb the protein under investigation, and the ability of nitriles to accept hydrogen bonds, which causes frequency shifts that are not described by the Stark effect. The consequence of this is that vibrational spectroscopy of nitriles in biomolecules could be predominately sensitive to their local hydration status, not electrostatic environment, and have the potential to be particularly destabilizing to the protein. Here, we introduce green fluorescent protein (GFP) as a model system for addressing these concerns using biosynthetically incorporated *p*-cyanophenylalanine (pCNF) residues in the interior of GFP and measuring absorption energies of both the intrinsic GFP fluorophore and *p*CNF residues in response to a series of amino acid mutations. We show that observed changes in emission energy of GFP due to the mutations strongly correlate with changes in electric field experienced by both the nitrile probes and the intrinsic fluorophore. Additionally, we show that changes in electric field measured from the intrinsic fluorophore due to amino acid mutations are unperturbed by the addition of *p*CNF residues inserted nearby. Finally, we show that changes in electric field experienced by the vibrational probes trend monotonically with changes in field experienced by the native fluorophore even though the nitrile probe is engaged in moderate hydrogen bonding to nearby water molecules, indicated by the temperature dependence of the nitrile's absorption energy. Together these results demonstrate that even in the presence of hydrogen bonding it is possible to relate nitrile absorption frequencies to electrostatic environment by comparing highly similar environments. GFP's intrinsic linear sensitivity to electric fields makes it a convenient model system for studying electrostatics in proteins that offers lessons for proteins without this visible fluorophore.

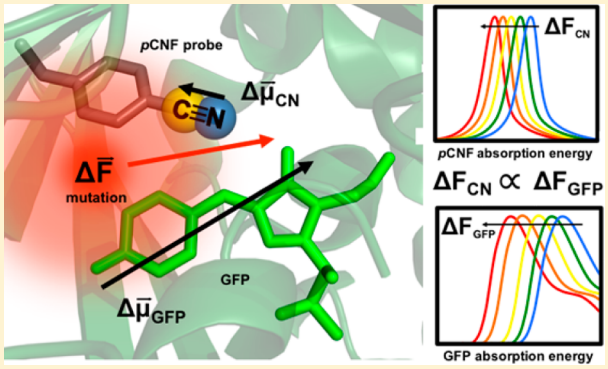

INTRODUCTION

Electrostatic fields generated by the three-dimensional distribution of partial charges throughout a structured protein provide a fundamental link between amino acid sequence and function including folding, reactivity, kinetics, and multimolecular interactions.[1−6] Understanding this link enables designing enzymes with improved functions, understanding and combating diseases, and providing benchmarks for computational models that accurately calculate electrostatic fields. Traditionally, electrostatic environments in proteins have been sensed indirectly via observed shifts in ^{19}F NMR signals[7,8] or side chain pK_as.[9−12] However, because of the complexity of proteins and the long-range nature of electrostatic forces, the interpretation of these experiments can be ambiguous and indirect. In contrast, the Stark effect has been a convenient theoretical framework for directly measuring electric fields in a wide range of biological contexts. In general, the Stark effect refers to the change in absorption energy, ΔE, of a chromophore in response to an applied electric field, $\Delta\vec{F}$, based on eq 1.

$$\Delta E = -(\Delta\vec{\mu}\cdot\Delta\vec{F} + \Delta\vec{F}\cdot\Delta\alpha\cdot\Delta\vec{F} + ...) \quad (1)$$

The change in absorption energy can be described by a Taylor series expansion about the applied electric field, which is generally truncated after two terms. The linear term depends on the difference dipole moment, $\Delta\vec{\mu}$, i.e., the difference in dipole moment between the ground and excited states involved in the transition. The quadratic term depends on the difference polarizability, $\Delta\alpha$, which refers to the change in polarizability between the two states of the chromophore in the direction of

Received: February 26, 2016
Published: April 29, 2016

DOI: 10.1021/jacs.6b02156
J. Am. Chem. Soc. 2016, 138, 6561−6570

the transition moment. Conveniently, most vibrational transitions are accompanied by negligible changes in polarizability, and so vibrational Stark effects are generally dominated by the linear term in eq 1 and can be reduced to eq 2, where $\Delta F_{||}$ is the component of the total field change projected onto the vector $\Delta\vec{\mu}$.

$$\Delta E = hc\Delta\upsilon = -\Delta\vec{\mu}\cdot\Delta\vec{F} = -f\Delta\mu\Delta F_{||} \quad (2)$$

Here, f represents the local field correction factor, which can be approximated as a scalar and is generally thought to have a value between 1 and 2.[13]

Vibrational Stark effect (VSE) spectroscopy, in which changes in vibrational frequencies, $\Delta\nu$, are interpreted in terms of electric fields based on eq 2, has become a widely used technique to study electrostatics in many biological contexts.[14−20] Once the value of $\Delta\vec{\mu}$, also called the Stark tuning rate, of a chromophore has been calibrated in an applied electric field of known magnitude, changes in its absorption energy can be used to calculate $\Delta F_{||}$, the change in electric field in the direction of $\Delta\vec{\mu}$, due to specific perturbations to the protein or environment. VSE spectroscopy has proven to be useful for measuring changes in electric fields caused by many types of perturbations including protein binding,[16,17,21,22] ligand binding,[13,23] amino acid mutation,[24] and location-dependent changes.[15,25,26] To facilitate studies of this nature, many vibrational probe groups have been developed, including azides, carbonyls, C−D bonds, and nitriles.[14,27]

Nitrile VSE probes are of particular interest because of their relatively large $\Delta\vec{\mu}$ values (0.4−0.8 $cm^{-1}/(MV/cm)$), large absorptivity ($\varepsilon \sim 500\ M^{-1}\ cm^{-1}$), and absorption in a region of the infrared well removed from a protein's background vibrations ($\upsilon_{CN} \sim 2100-2240\ cm^{-1}$).[14,28] To facilitate these experiments, a number of methods for incorporating nitriles into proteins or peptides have been developed, such as chemical synthesis, posttranslational modification, or nonsense suppression. Additionally, because $\Delta\vec{\mu}$ for the nitrile stretch is parallel to the nitrile bond vector, the measured change in absorption energy can be directly related to the change in field in the direction of the nitrile bond. The utility of nitrile probes is diminished, however, by their ability to accept hydrogen bonds, which, while being electrostatic in origin, causes deviation from the Stark effect model due to quantum effects associated with the hydrogen bond. Indeed, it has been shown in non-hydrogen bonding solvents that the nitrile frequencies of acetonitrile and benzonitrile are inversely proportional to solvent dielectric.[29,30] However, in water and other protic solvents, the frequencies are not well correlated with solvent dielectric or any other solvent property.[31,32] Ab initio calculations of acetonitrile and methyl thiocyanate in water have also revealed that nitrile frequencies can span as much as 25 cm^{-1} depending on the geometry of the hydrogen bond between nitrile and water.[33] This sensitivity to hydrogen bonding, which arises from changes in the force constant of the nitrile bond upon hydrogen bonding rather than changes in the difference dipole moment, casts doubt on the efficacy of nitriles as VSE probes of electric field. This is a major concern when attempting to compare experimentally measured frequencies to electric fields calculated from simulations,[34−36] and several attempts have been made to deconvolute these competing effects. Fafarman et al., have shown that by comparing nitrile frequencies to chemical shifts of isotopically labeled nitriles, it is possible to subtract the hydrogen bonding contribution to the frequency and determine the portion of a frequency shift that is only due to electrostatic field effects.[37] However, in spite of this advancement in the interpretation of nitrile VSE experiments, there is still not agreement on the ability of nitrile frequencies to report directly on electric fields. For example, it has been suggested that nitrile stretches in biological systems are predominantly sensitive to their local hydration status and are most useful for determining if a particular position is buried or solvent exposed.[35,38]

Furthermore, the ability of nitriles to accept hydrogen bonds leads to the possibility of introducing hydrogen bonds where there previously were none. This could grossly misrepresent the behavior of the native system, the understanding of which is the ultimate goal. Adhikary et al., have shown that nitrile probes can be particularly destabilizing, with buried probes causing more destabilization than solvent-exposed ones.[35] This measure of protein destabilization due to a nitrile probe represents an attempt to quantify the amount of perturbation due to the probe, which is an effect that needs to be investigated whenever a non-native probe is used to interrogate a system. For proteins it is common to assay the function with and without the probe, and as long as the function is not altered significantly it is assumed that the probe does not significantly perturb the system under investigation.[13,17,24] However, measurements like these only indirectly assess the extent of perturbation caused by the probe. If the insertion of a nitrile probe drastically perturbs the electrostatic environment of the protein, for example by the addition of its large ground state dipole moment, then electric field measurements based on the nitrile probe frequencies are not likely to lead to any understanding of the electrostatics in the native protein. Additionally, it is possible that an electrostatic probe could cause local perturbations in electrostatic field without affecting the observed structure, stability, or function, and so an assay of any of these properties would not reveal problematic changes caused by the nitrile itself. In the case of a site-specific nitrile VSE probe, it would be desirable to know what the electrostatic field is in the absence of the probe.

In the work presented here, we use green fluorescent protein (GFP), whose intrinsic fluorescent chromophore serves as a visible Stark effect probe of electric field, as a model system to directly measure the extent of electrostatic perturbation caused by nitrile probes introduced on the artificial amino acid *p*-cyanophenylalanine (*p*CNF). GFP, shown in Figure 1, is one of the most widely used and well-studied proteins due to its unique fluorescence, which is a result of protein folding and does not depend on any cofactor binding or other external modification.[39,40] Upon protein folding in the presence of oxygen, the side chains of residues 65, 66, and 67 (threonine, tyrosine, and glycine, or TYG, in the wild type) autocatalytically form the fluorophore, which has two major absorption peaks at 395 and 480 nm, depending on whether the tyrosyl oxygen of residue 66 is protonated or deprotonated, respectively.[39,41,42] In wild type GFP, absorption of either of these forms of the fluorophore results in emission at ∼510 nm with a high quantum yield.[39] However, many mutations have been made to wild type GFP to shift the emission energy, and to optimize other properties such as folding rate, stability, and quantum yield, for fluorescence microscopy experiments.[43−46]

In particular, the side chain of T203 is optimally oriented such that its replacement with an aromatic residue forms a stabilizing interaction with the fluorophore that shifts the emission to lower energy. Indeed, it has been shown that incorporating different residues at position 203 can shift the

DOI: 10.1021/jacs.6b02156
J. Am. Chem. Soc. 2016, 138, 6561−6570

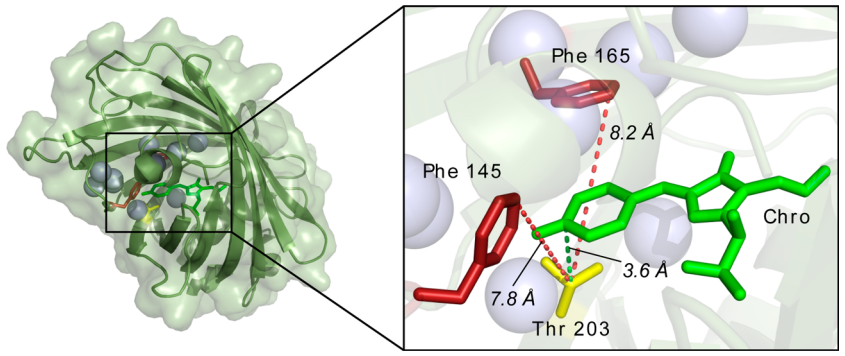

Figure 1. Crystal structure of superfolder GFP (PDBID: 2B3P). The backbone is shown as a ribbon structure and the solvent accessible surface area is shown as a light green surface. Phe 145 and 165 are shown in red, Thr 203 is shown in yellow, and the fluorophore is shown in green. Eight ordered waters that are <7 Å from either residue 145 or 165 are shown as light blue spheres.

emission by as much as 20 nm.[45] In addition to this emission sensitivity, it has been shown that the deprotonated absorption band (hereafter referred to as the B state) of the TYG fluorophore is linearly sensitive to applied electric fields based on the Stark effect with a negligible quadratic term (eq 2).[47] Here, we have chosen to work with superfolder GFP (hereafter simply referred to as GFP), which was designed to have optimum pH stability and quantum yield, minimal propensity for aggregation, and the ability to fold quickly and remain stable when tagged to a poorly folding protein.[48] This version of GFP also contains the TYG fluorophore, whose intrinsic linear sensitivity we exploit in this work.

By making use of a system that contains both a vibrational (*p*CNF) and an electronic (GFP fluorophore) Stark effect probe, we investigated whether these probes gave a similar electrostatic response to the same set of perturbations. Additionally, GFP's intrinsic linear sensitivity to electric field makes it useful as a model system for addressing the aforementioned challenges of using nitriles as Stark effect probes. Using nonsense suppression,[49,50] we inserted *p*CNF residues at positions 145 and 165 near the GFP fluorophore (Figure 1) and measured changes in absorption energy of these vibrational and electronic chromophores in response to a series of mutations to position 203. We found that the change in fluorescence wavelength of GFP is strongly correlated to electric fields measured from both the vibrational and electronic Stark effect probes, and that similar types of mutations project similar changes in field onto all of the chromophores. In addition, we used the GFP fluorophore to measure the extent of electrostatic perturbation caused by the *p*CNF probes. We observed that nitriles at these two locations can introduce changes in electrostatic environment around the TYG fluorophore, but that the changes are systematic and do not affect the fluorophores's intrinsic sensitivity to mutations at position 203. Additionally, temperature dependent FTIR spectra of the nitrile-containing proteins suggest that the *p*CNF residues participate in hydrogen bonds even when buried in the interior of the protein. The observation that these nitrile probes give the same response as an independent field reporter to a series of mutations while engaging in hydrogen bonding suggests that Stark effect spectra of similar states may still be interpreted in electrostatic terms. While GFP is unique because of its intrinsic fluorophore, this work serves as an important example of how VSE of nitrile probes may be applied to other proteins of interest.

EXPERIMENTAL METHODS

Expression and Purification of GFP Mutants. Plasmids containing the genes for wild type GFP (pBAD-GFP) and an orthogonal nonsense suppressor pair for *p*CNF (pDULE-*p*CNF) were a generous gift from the Mehl laboratory.[51] Site-directed mutagenesis (Stratagene) was used to make mutations to the pBAD-GFP plasmid at amino acid positions 145, 165, and 203. GFP constructs with no nitrile probe contained only the position 203 mutations and were transformed into DH10β cells. GFP constructs containing a nitrile probe were mutated to contain a rare stop codon (TAG in one-letter nucleotide code) at either position 145 or 165 and were cotransformed with the pDULE-*p*CNF plasmid into DH10β cells. Single colonies from these transformations were used to seed 5 mL cultures that grew for 16 h in LB media at 37 °C. 2.5 mL of these cultures was used to seed 1 L of autoinduction media, as detailed by Hammill et al.[52] The cotransformed cells were supplemented with 1 mM *p*CNF. After 25–30 h at 37 °C, the cells were collected by centrifugation, purified by immobilized metal affinity chromatography, and the affinity tags were cleaved as described elsewhere.[48] After purification, protein masses were verified by FPLC-MS and the verified protein was buffer exchanged into PBS (pH = 7.4) and concentrated to 2 mM for spectroscopic experiments.

Absorption and Fluorescence Spectroscopy. UV–vis absorption scans were performed using a Cary 5000 spectrometer and a 1 cm quartz cuvette. Circular dichroism spectra were collected on a Jasco J-815 spectrometer using a 1 mm quartz cuvette and averaging over 10 scans. All FTIR spectra were collected using a Bruker Vertex 70. The sample was injected into a cell between two sapphire windows separated by 125 μm Teflon spacers, and 250 scans were collected with a resolution of 0.5 cm^{-1}. Temperature dependent FTIR spectra were collected in a similar cell with 100 μm Teflon spacers. 200 scans were collected for *p*-tolunitrile in solvent and 600 scans were collected to achieve an adequate signal-to-noise ratio for the *p*CNF-containing proteins. Spectra were baseline-corrected using an in-house fitting program described previously.[17] *p*-Tolunitrile and all solvents were purchased from Sigma and used without further purification. Fluorescence spectra were collected from samples in 1 cm polystyrene cuvettes with a Fluorolog3 spectrometer using a 1.5 nm slit width and a spectral resolution of 0.1 nm. All absorption and fluorescence measurements were averaged over at least three individual measurements.

RESULTS AND DISCUSSION

By incorporating nitrile probes near the fluorophore of GFP, we sought to compare the response of the vibrational and electronic chromophores to the same set of perturbations. First, we compared the changes in electric field measured from both the vibrational and electronic chromophores and found that they are in excellent agreement. Next, by comparing the changes in emission energy of the fluorophore with and without

DOI: 10.1021/jacs.6b02156
J. Am. Chem. Soc. 2016, 138, 6561–6570

*p*CNF, we directly assessed the extent of electrostatic perturbation due to the inclusion of the *p*CNF probe itself. Finally, through a series of measurements of the temperature dependence of nitrile frequencies, we examined whether the inserted *p*CNF residues engaged in a moderate amount of hydrogen bonding even when confined to the interior of the *β*-barrel, and discuss the implications of this on the interpretation of vibrational Stark effect spectra.

We measured frequency changes of *p*CNF residues at two interior locations of GFP (positions 145 and 165), as well as frequency changes in both the absorption and emission of the deprotonated fluorophore, in response to five amino acid substitutions at position 203. Because the emission wavelength of GFP is known to be especially sensitive to mutations of amino acid 203, we reasoned that T203X mutations (where T is the original amino acid at position 203 and X represents the new amino acid: S, N, H, F, or Y) would create large changes in electric field that could be measured by both the electronic and vibrational chromophores. We chose positions 145 and 165 to insert the *p*CNF probes because the native phenylalanine side chains are optimally oriented on either side of the interaction between residue 203 and the fluorophore, and molecular modeling showed that nitriles at the *para* positions of the phenyl rings would point toward the fluorophore. Figure 2

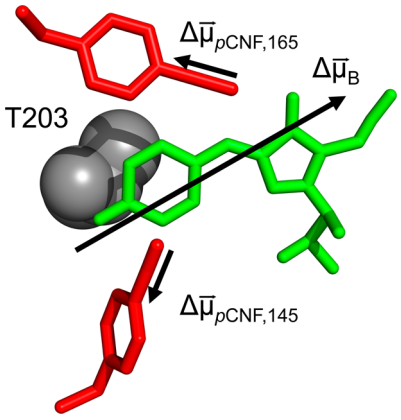

Figure 2. Close up view of crystal structure 2B3P highlighting Phe 145 and 165 (red), the GFP fluorophore (green), and Thr 203 (gray). Arrows represent the approximate magnitudes and directions of difference dipole moments of *p*CNF residues inserted at position 145 or 165, as well as the B state of the GFP fluorophore.

shows crystal structure 2B3P with *p*CNF residues modeled into positions 145 and 165. The arrows represent $\Delta\vec{\mu}$ vectors, which point from nitrogen to carbon on the nitrile probes and from the hydroxyl group to the imidazolidone ring of the fluorophore. Additionally, Phe residues at these two positions are oriented nearly identically across several crystal structures containing the above T203X mutations, which suggests that *p*CNF residues inserted there might have a small range of motion.[39,53] As the Stark effect model allows us to interpret frequency changes as changes in field projected along a probe's difference dipole moment, it is desirable that the probe be as stationary as possible because the field projection depends on the probe's orientation in the field.

Representative spectra for the absorption of *p*CNF 145 GFP mutants, as well as absorption and emission of the intrinsic fluorophore are shown in Figure 3, and representative spectra for *p*CNF 165 mutants are shown in Figure S1 of the

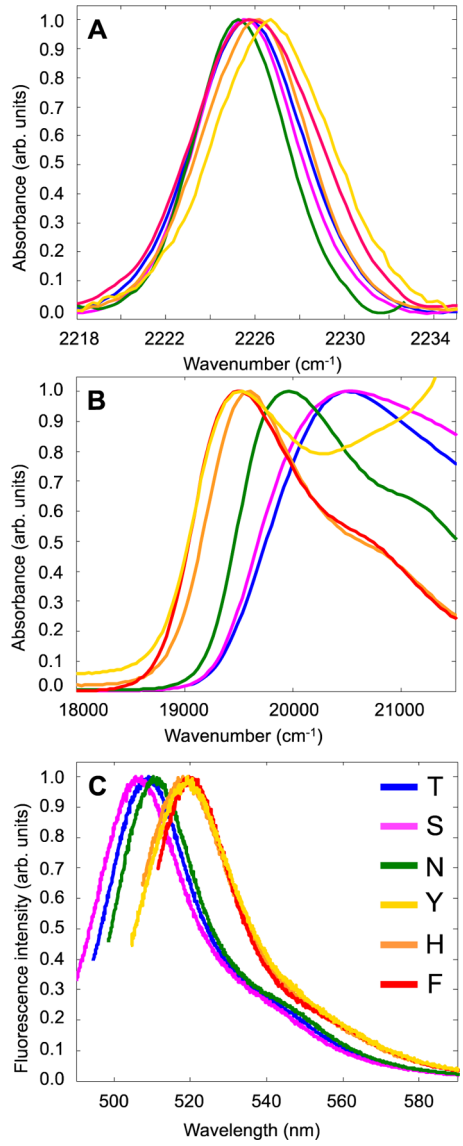

Figure 3. Representative spectra of nitrile-containing GFP constructs. (A) Nitrile 145 absorption; (B) fluorophore absorption; and (C) fluorophore emission. Colors represent a different amino acid at position 203 based on the one letter amino acid codes shown inside panel (C).

Supporting Information. As seen in Figure 3A, the FTIR spectra of the position 145 nitrile were well-described by a single Gaussian function with a fwhm of roughly 5−6 cm^{-1} (with the exception of the T203F mutant), which is similar to that for the free amino acid in a low dielectric solvent like THF.[31] Along with published crystallographic evidence, the narrow width of these bands suggests that each *p*CNF residue is likely confined to a region of space where it only sees a single, well-defined environment. For each nitrile position, the maximum shifts observed were on the order of 2 cm^{-1}. The absorption bands of the deprotonated fluorophore (Figure 3B) also exhibited a strong dependence on the T203X mutations, with maximum shifts on the order of ∼1000 cm^{-1}. There was also more variability in the width of these bands. We observed narrower absorption peaks when the bulkier, aromatic residues (F, Y, and H) were at position 203, while the peaks were generally broadened when the smaller, polar side chains (T and S) were at position 203. This likely reflects a change in the pK_a

DOI: 10.1021/jacs.6b02156
J. Am. Chem. Soc. 2016, 138, 6561−6570

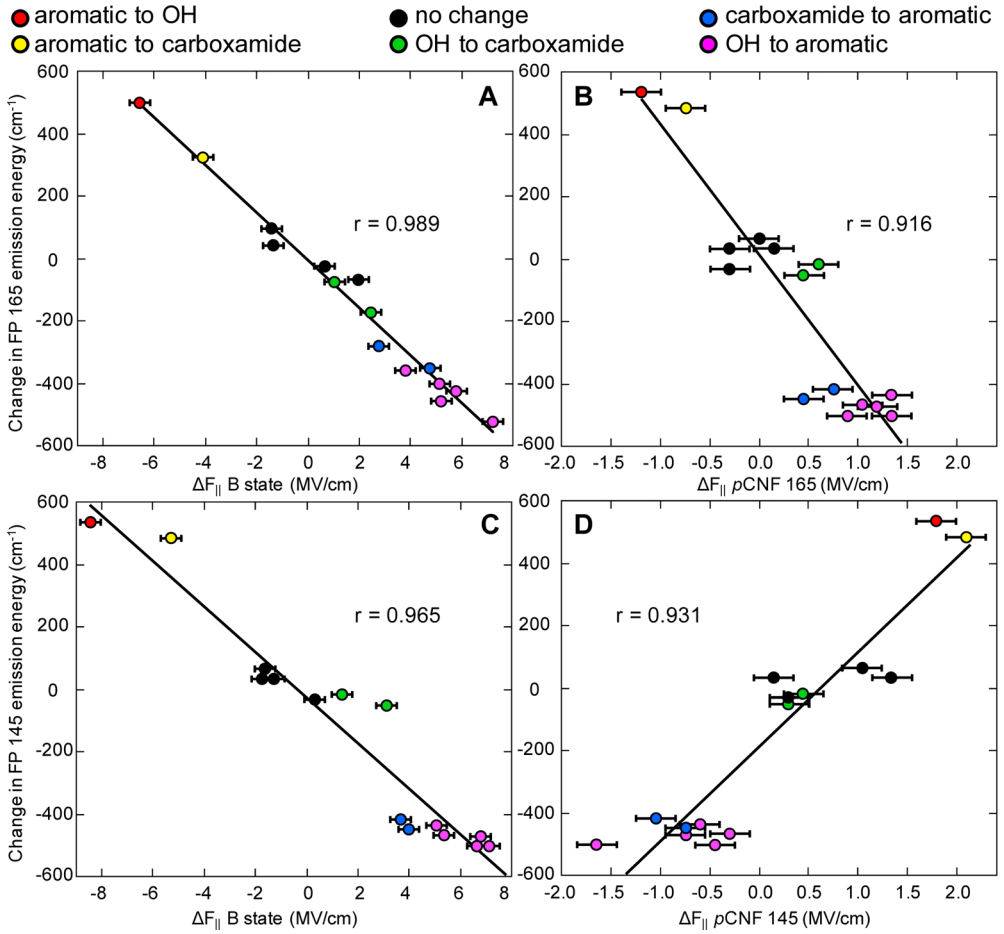

Figure 4. Change in the emission energy of the intrinsic fluorophore plotted against the change in field, calculated from B state absorption energies (A, C) or *p*CNF absorption energies (B, D), in response to mutations at position 203. The 15 data points on each plot are derived from the total number of energy differences between the six T203X mutant energies. The values of $\Delta F_{\|}$ on the *x*-axes are electric field projections calculated from eq 2. On the *y*-axes, FP stands for fluorescent protein. Colors represent the type of mutation at position 203. Error bars represent the maximum error based on standard deviations in published Stark tuning rates. The slopes of the best-fit lines (in $cm^{-1}/(MV/cm)$) are A: −76.3, B: −355.2, C: −72.8, D: 303.2.

of the fluorophore's tyrosyl oxygen, which causes a change in the relative populations of the A and B states and results in a broadened B state absorption. Shifts in pK_a such as these have been used previously to investigate electrostatic environments, and in future studies could prove to be a useful comparison to the frequency shifts measured here. Finally, representative emission spectra of the GFP variants are shown in Figure 3C, demonstrating that all mutations at T203X displayed the same major peak between 505 and 525 nm with a broader, less intense shoulder to the red.

Linking Vibrational and Electronic Stark Effects via GFP Fluorescence. The usefulness of GFP for these studies lies in the intrinsic fluorophore, whose B state absorption energies have been shown to trend linearly with electric field strength. This intrinsic electronic Stark effect probe has a measured Stark tuning rate of 117.5 $cm^{-1}/(MV/cm)$ oriented 21° away from the transition dipole moment, shown in Figure 2.[47,54] The Stark tuning rate of this electronic transition is much larger than that of the vibrational stretching transition of *p*CNF, which has a measured Stark tuning rate of 0.67 $cm^{-1}/(MV/cm)$.[55] In addition, because the emission wavelength is dependent on the complex noncovalent interactions around the fluorophore, it serves as a convenient probe to assess the effect of inserted *p*CNF probes on these interactions. We therefore wanted to use the emission wavelength of GFP to check the electrostatic responses of *p*CNF probes against those of the electronic fluorophore.

To measure the effect on electric field due to T203X mutations, we have compared the changes in emission energy of the fluorophore between all pairs of mutants against the projection of changes in field onto either the vibrational or electronic probe ($\Delta F_{\|}$ from eq 2, where the local field factor is assumed to be 1). Here, the six different T203X mutants give rise to 15 individual differences in energy. This is seen in Figure 4, where we plot the changes in emission energy against the corresponding change in electric field, measured from either the *p*CNF probes or the GFP fluorophore. Figure 4A and 4B show the changes in emission energy plotted against the field changes projected onto the electronic and vibrational chromophores, respectively, for the mutants containing *p*CNF at position 165. Similarly, Figure 4C and 4D show the same data measured for the mutants containing *p*CNF at position 145. As can be seen in Figure 4A–D, changes in the observed fluorescence are strongly correlated with changes in electric field measured from both *p*CNF probes and the fluorophore, with $r > 0.91$ for all comparisons. The size of the error bars is not indicative of variability in the peak centers of the fluorophores, which remained remarkably constant across replicate measurements

DOI: 10.1021/jacs.6b02156
J. Am. Chem. Soc. 2016, 138, 6561−6570

(standard deviations were ∼0.05 cm^{-1} for all *p*CNF probes and ∼0.1 nm for the GFP fluorophore, determined by at least three measurements of each). Rather, the size of the error bars is a result of both the uncertainty in the calibrated Stark tuning rates and the resolution of the UV−vis and FTIR spectrometers. The difference in sign on the slopes of the two plots in Figure 4B and 4D, measured from the *p*CNF probes, as well as their different magnitudes along the *x*-axis, highlights the spatial dependence of energy changes based on eq 2. Because *p*CNF 145 and *p*CNF 165 are oriented differently in space (Figure 2), projections of the same field onto their respective bond axes are not expected to give the same value or sign of field, which in this case is revealed by the differing signs of the slopes.

In addition to the strong correlation of color and electric field from each location, the data were grouped into clusters based on the molecular identity of the mutations. Of the six amino acid side chains that we placed at position 203, we grouped each based on being aromatic (Phe, Tyr, and His), polar with an −OH group (Ser and Thr), or polar with a carboxamide group (Asn). The color scheme in Figure 4 represents different types of mutations based on this grouping of side chains. It is important to note that in Figure 4 (and the following figures) data describing opposite mutations (i.e., "aromatic to OH" and "OH to aromatic") are not simply derived from the same mutation with the order of subtraction reversed. The data points arising from the apparent order change are unique, for example: Tyr to Ser versus Thr to Phe. It is not clear a priori that these two mutations should cause approximately the same magnitude shift in the opposite direction, and thus the observation that they do is significant. Furthermore, we tested the effect of manipulating the data sets so that the subtraction was done in the same way every time (e.g., only OH to aromatic). However, doing this did not result in any significant changes to the trends that we observed (data not shown), nor did it have any effect on the conclusions we draw from these studies.

Cataloging His and Tyr by this scheme was somewhat ambiguous due to the presence of an −OH group on Tyr and the possibility of His to be charged and not aromatic. However, we reasoned that because mutations involving these side chains were closer in energy to aromatic mutations (vida infra), His 203 is not charged and the aromatic ring is more important than the hydroxyl group for the interaction between the fluorophore and Tyr 203. Indeed, previous measurements of the pK_a of His 203 have indicated that it is not charged at neutral pH.[56] Figure 4 clearly shows that when grouped in this way, similar types of mutations caused similar changes in field and emission energy regardless of which chromophore (electronic or vibrational) was being used to measure the field change. These results unambiguously demonstrate that the two Stark chromophores responded identically to the same electrostatic perturbations caused by mutations at position 203, independent of the exact transition being measured or position of the probe within the <10 Å diameter region we investigated (Figure 1). This further suggests that the non-native *p*CNF probes can be inserted near the GFP fluorophore without disrupting its intrinsic sensitivity to nearby mutations.

Electrostatic Perturbation Due to pCNF Probes. Interest in using the nitrile as a vibrational Stark probe has occasionally been tempered by the worry that the large ground state dipole moment of the oscillator itself (∼4 D) could disrupt the local electrostatic environment of a biomolecule to such a great extent that the label could invalidate the measurement. A necessary step in the interpretation of nitrile frequencies in terms of electric field changes is the quantification of the perturbation due to the nitrile-containing probe, which is often indirectly assessed through functional assays or thermal stability measurements. If an inserted nitrile probe does not greatly alter protein function or stability, measured through a thermodynamic or kinetic parameter, then it is assumed that the environment around the probe must not have been very affected by the insertion of the probe. While the stability and function of a protein are undoubtedly linked to local electrostatic environment, they are not direct reporters of it. Even in the instance that a crystal structure can be determined for both native and probed proteins, electrostatic information is exceedingly difficult to interpret from structural data.[57]

With GFP, the presence of an intrinsic fluorophore formed through protein folding provides an independent handle to investigate any possible alteration of the electrostatic environment caused only by the insertion of the *p*CNF probes themselves. We therefore measured the changes in field experienced by the GFP fluorophore in response to the insertion of *p*CNF at either position 145 or 165. Figure 5 shows

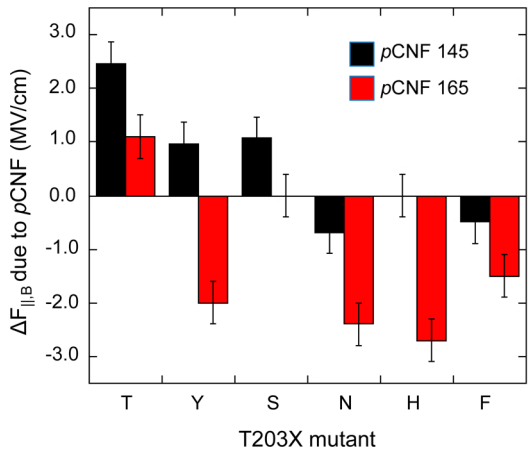

Figure 5. Change in field experienced by the B state of the GFP fluorophore, due to the insertion of *p*CNF probes at either position 145 or 165. The *x*-axis denotes the identity of the residue at position 203 by its one letter amino acid code. Error bars represent the maximum error based on standard deviations in published Stark tuning rates.

the magnitude of this field change (calculated from eq 2) for each of the six T203X variants when *p*CNF was inserted at either position 145 or 165. For nearly all of the T203X mutants, the insertion of a nitrile probe at either position induced a change in field of up to ±3 MV/cm relative to the wild type fluorophore. However, when we compared the changes in fluorophore emission energy to changes in field measured by the electronic fluorophore with and without the nitrile probes (Figure 6), it is clear that the nitrile probes do not affect the intrinsic fluorophore's sensitivity to the T203X mutations. In this instance, the changes in field experienced by the fluorophore due to the T203X mutations (circles) are independent of either inserted nitrile probe (squares or diamonds). Furthermore, the same patterns of functional groups of the side chain at position 203 were preserved compared to Figure 4. These results together suggest that

DOI: 10.1021/jacs.6b02156
J. Am. Chem. Soc. 2016, 138, 6561−6570

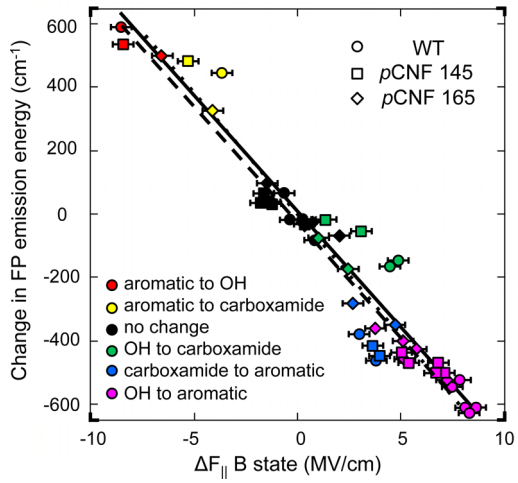

Figure 6. Change in emission energy due to position 203 mutation plotted against the change in field of the B state of the fluorophore, with (squares and diamonds) and without (circles) *p*CNF probes. The values of $\Delta F_{||}$ on the *x*-axis are electric field projections calculated from eq 2. On the *y*-axis, FP stands for fluorescent protein. Colors represent the type of mutation at position at 203. Best-fit lines are shown in black for wild type (solid line; $r = 0.960$), *p*CNF 145 (dashed line; $r = 0.965$), and *p*CNF 165 (dotted line; $r = 0.989$). Error bars represent the maximum error based on standard deviations in published Stark tuning rates.

*p*CNF probes, while causing changes in the absolute value of the electric field in their immediate environment, do not affect the response of the native protein to changes in field caused by nearby mutations. This result is significant, because while the determinants of the nitrile oscillation frequency may be too complicated for it to report absolute values accurately, it appears to be an unobtrusive reporter of changes between two similar environments. The latter of which is by far the most common application of vibrational Stark effect spectroscopy.

Vibrational and Electronic Field Reporters Agree Even in the Presence of Hydrogen Bonding. The final issue we sought to investigate with the comparison of vibrational and electronic chromophores is the effect of hydrogen bonding on the vibrational Stark effect spectra of nitriles. There has been significant recent debate over the utility of nitrile vibrations as electric field reporters in the presence of hydrogen bonding, which is known to shift the oscillator vibration to higher energy.[29,32,35,37,58−60] It has been demonstrated that this shift can be deconvoluted into hydrogen bonding and Stark effects in water using independent ^{13}C NMR measurements in concert with vibrational spectroscopy; however, this has not been demonstrated in solvents other than water.[37] Because of this, it has been suggested that because of their predominate sensitivity to hydration, the interpretation of nitrile frequencies in terms of electric fields via eq 2 requires that the nitrile be free of hydrogen bonding.[61] If true, this would significantly limit the utility of nitriles through the vibrational Stark effect in biological systems. GFP is an excellent example of this; although the nitrile chromophore was inserted at positions in the protein interior, multiple crystal structures of GFP clearly reveal significant quantities of water inside the β-barrel of the protein, some of which is shown in Figure 1. If the nitrile chromophore cannot be used in such a nominally solvent-sequestered environment, its utility in general will be very limited.

To investigate this problem in the GFP system, in Figure 7 we have compared the changes in electric field, measured from both of the *p*CNF probes and the intrinsic fluorophore absorption, in response to the T203X mutations. If hydrogen bonding to the nitrile probes rendered them ineffective as electric field probes, then we would not expect good correlation between the measured frequencies of the vibrational and electronic chromophore absorptions because additional physical effects besides electric field would be convoluted into energy shifts of the nitriles. However, Figure 7 shows that from both nitrile probe locations, we observed a monotonic trend between the changes in field measured from the vibrational reporter and those from the electronic reporter with high correlation constants ($r > 0.87$ in both cases). This finding suggests one of two possibilities: (a) that neither of the *p*CNF probes formed hydrogen bonds with water or nearby protein atoms, or (b) that one or both of the *p*CNF probes did engage in hydrogen bonds but that this did not affect the ability of either of these probes to report on changes in electric field. While it seems likely, by inspection of crystal structures (Figure

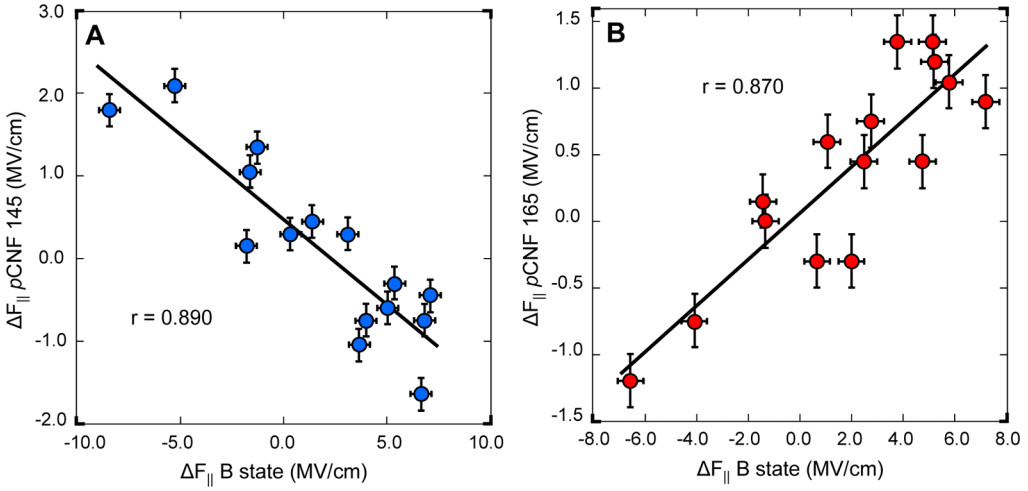

Figure 7. Comparison of changes in field measured from *p*CNF probes (A: 145; B: 165) and B state of GFP fluorophore. The values of $\Delta F_{||}$ on the *x*- and *y*-axes are electric field projections calculated from eq 2. Error bars represent the maximum error based on standard deviations in published Stark tuning rates. The slopes of the best-fit lines are (A) −0.206 and (B) 0.173.

DOI: 10.1021/jacs.6b02156
J. Am. Chem. Soc. 2016, 138, 6561−6570

1), that a *p*CNF inserted at either location 145 or 165 engages in hydrogen bonding due to the abundance of nearby water molecules at these positions, it is worthwhile to further investigate the hydrogen bonding status of nitriles at these positions due to the possible implication of this for the interpretation of Stark effect spectra.

Recently, Adhikary et al. have reported a straightforward method for determining the hydrogen bonding status of nitrile probes based on the temperature dependence of vibrational frequencies through a frequency-temperature line slope (FTLS).[61] It was shown that the magnitude of the FTLS is unique for small nitriles in a variety of protic and aprotic solvents, and that the model nitrile data can be used to assess the hydrogen bonding status of nitrile probes inserted at various locations in a protein. Here we used the same analysis for *p*CNF, *p*-tolunitrile, and GFP mutants containing *p*CNF at positions 145 and 165. Figure 8 shows the change in frequency

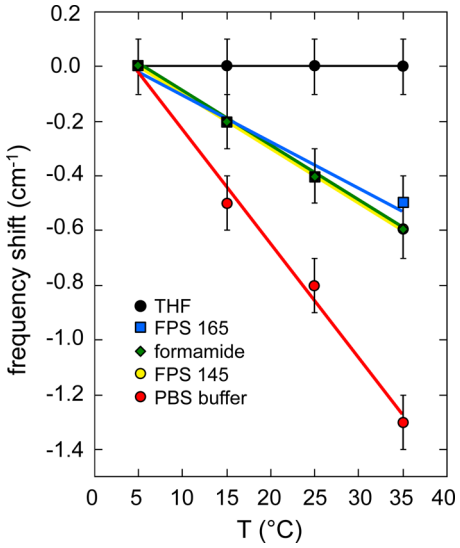

Figure 8. Changes in nitrile stretching frequency (relative to the value at 5 °C) as a function of temperature. Black, green, and red data points represent the frequency of *p*-tolunitrile in the noted solvent (or *p*CNF, in the case of PBS buffer). Blue and yellow data points are GFP T203S constructs that contain *p*CNF at position 165 or 145, respectively. Error bars represent the instrument resolution. Standard deviations across at least three measurements were ~0.05 cm^{-1} for all nitriles.

as a function of temperature for small nitriles in three solvents, as well as *p*CNF 145 and 165 for the T203S GFP mutants. Again, the error bars are indicative of the instrument resolution and not the variability across multiple measurements. Similar to previous reports, we observed characteristic FTLSs of *p*-tolunitrile and *p*CNF when dissolved in an aprotic solvent (THF, black), a moderate hydrogen bonding solvent (formamide, green), and water (red), with the magnitude of the FTLS increasing in that order. These data were then compared to the temperature dependent spectra of two constructs of GFP containing a *p*CNF residue at either position 145 (yellow) or 165 (blue). For both nitrile locations, the FTLSs were very similar to that of the small molecule in formamide, which suggests that they experienced a moderate amount of hydrogen bonding in GFP. This observation for the position 145 nitrile is interesting, because its low frequency would ordinarily suggest a lack of hydrogen bonding based on the well-known shift to higher frequency upon the acceptance of a hydrogen bond.[31,32] However, Cho et al. have shown that the nitrile frequency can span ~25 cm^{-1} depending on the geometry of the hydrogen bond.[33] It seems likely to us that *p*CNF 145, being shielded from the solvent and exposed to confined water molecules, might be forced to adopt a hydrogen bonding geometry that gives rise to the observed low frequencies. Further high resolution structural studies are being pursued to provide insight into this interesting observation.

To rule out the possibility of subtle structural changes to GFP causing the observed frequency shifts, we recorded circular dichroism spectra of WT and *p*CNF 165 over this small temperature range (Figure S2). Over this temperature range, GFP did not have any measurable change in secondary structure, which suggests that the observed FTLSs of *p*CNF 145 and 165 are indicative of moderate hydrogen bonding. This result supports our hypothesis from crystallographic data that nitriles at these two positions are likely to engage in hydrogen bonding, probably from water molecules contained within the β-barrel structure of GFP. In the crystal structure shown in Figure 1, as well as others that have been solved for similar constructs of GFP, positions 145 and 165 are entirely shielded from bulk solvent but are in close proximity to several confined water molecules. Together these data suggest that *p*CNF probes at these locations participate in hydrogen bonding, and yet still accurately report on changes in field as measured from the electronic fluorophore.

This finding is significant because it suggests that it is possible to relate changes in the absorption energies of nitrile probes to changes in electric field, even in the presence of hydrogen bonding. This result is similar to the conclusion reached by Fafarman et al., where nitrile probes exposed to bulk water had frequencies that were all shifted by a constant 10 cm^{-1} with respect to an independent NMR parameter.[37] In the present study, there appears to be a constant contribution to the nitrile frequency from the hydrogen bonds to ordered water molecules that cancels out when comparing two similarly hydrogen bound nitriles. This suggests that small changes in the hydrogen bonding status of the nitrile probe between two states could still cause significant deviations from the Stark effect. In order to observe this independence of the frequency change on hydrogen bonding, it may still be necessary to compare states that are highly similar with respect to the hydrogen bonding status of the nitrile. Further studies are underway to compare Stark effects of the GFP fluorophore to nitrile frequencies of *p*CNF probes inserted into different positions with potentially different hydrogen bonding environments to assess the generality of this finding.

■ CONCLUSION

We have used GFP to explore the behavior of the nitrile vibrational Stark probe in comparison to the known visible Stark behavior of GFP's intrinsic fluorophore. Nitrile probes were inserted at buried locations near the fluorophore without affecting the sensitivity of the observed fluorescence to electrostatic changes made in the vicinity of the fluorophore by amino acid mutations. Additionally, changes in both the intrinsic fluorescence and site-specific electric fields were related to chemical properties of the amino acids involved in the mutations. We have also shown that the changes in absorption frequency of the two *p*CNF probes inserted at positions 145 and 165 caused by these same amino acid mutations resulted in changes in electric field that correlated

DOI: 10.1021/jacs.6b02156
J. Am. Chem. Soc. 2016, 138, 6561−6570

highly with electric fields measured independently from the electronic fluorophore.

A series of measurements of the temperature dependence of the nitrile frequencies suggests that they participate in hydrogen bonds with ordered water molecules inside the β-barrel. This result is not surprising, but is interesting because hydrogen bonding has been thought to complicate the interpretation of nitrile frequencies in terms of electric fields. However, pCNF probes at these two locations appear to accept hydrogen bonds, while simultaneously having absorption frequencies that are well described by the vibrational Stark effect. This suggests that it may not be necessary that a nitrile be free of hydrogen bonds in order to be useful as a Stark effect probe as long as differences in absorption energy between similar states are being considered. While GFP is almost unique in that the protein carries an intrinsic, easily measured electrostatic probe, the conclusions of this study can be generalized to nitriles used as vibrational probes in other proteins.

■ ASSOCIATED CONTENT

Supporting Information

The Supporting Information is available free of charge on the ACS Publications website at DOI: 10.1021/jacs.6b02156.

Figures S1 and S2. (PDF)

■ AUTHOR INFORMATION

Corresponding Author

*lwebb@cm.utexas.edu

Notes

The authors declare no competing financial interest.

■ ACKNOWLEDGMENTS

We would like to thank Dr. Ryan Mehl for providing us with the pBAD-GFP and pDule-pCNF plasmids. We are also grateful for the University of Texas Institute for Cell and Molecular Biology core facility for DNA sequence verification and protein mass analysis, and for the Texas Institute for Drug and Diagnostic Development for the use of their circular dichroism spectrometer. This work was supported by the Burroughs Wellcome Fund (1007207.01) and the Welch Foundation (F-1722).

■ REFERENCES

(1) Honig, B.; Nicholls, A. *Science* **1995**, *268* (5214), 1144−1149.
(2) Lee, L. P.; Tidor, B. *Protein Sci.* **2001**, *10* (2), 362−377.
(3) Villa, J.; Warshel, A. *J. Phys. Chem. B* **2000**, *105* (33), 7887−7907.
(4) Papazyan, A.; Warshel, A. *Curr. Opin. Struct. Biol.* **1998**, *8*, 211−217.
(5) Simonson, T. *Curr. Opin. Struct. Biol.* **2001**, *11* (2), 243−252.
(6) Gunner, M. R.; Nicholls, A.; Honig, B. *J. Phys. Chem.* **1996**, *100* (10), 4277−4291.
(7) de Dios, A. C.; Pearson, J. G.; Oldfield, E. *Science (Washington, DC, U. S.)* **1995**, *260* (5113), 1491−1496.
(8) Pearson, J. G.; Oldfield, E.; Lee, F. S.; Warshel, A. *J. Am. Chem. Soc.* **2013**, *115* (15), 6851−6862.
(9) Isom, D. G.; Castañeda, C. A.; Cannon, B. R.; García-Moreno, E. B. *Proc. Natl. Acad. Sci. U. S. A.* **2011**, *108* (13), 5260−5265.
(10) Dwyer, J. J.; Gittis, A. G.; Karp, D. A.; Lattman, E. E.; Spencer, D. S.; Stites, W. E.; García-Moreno, E. B. *Biophys. J.* **2000**, *79* (3), 1610−1620.
(11) Mehler, E. L.; Guarnieri, F. *Biophys. J.* **1999**, *77* (1), 3−22.
(12) Forsyth, W. R.; Antosiewicz, J. M.; Robertson, A. D. *Proteins: Struct., Funct., Genet.* **2002**, *48* (2), 388−403.
(13) Fried, S. D.; Bagchi, S.; Boxer, S. G. *Science* **2014**, *346* (6216), 1510−1514.
(14) Suydam, I. T.; Boxer, S. G. *Biochemistry* **2003**, *42* (41), 12050−12055.
(15) Shrestha, R.; Cardenas, A. E.; Elber, R.; Webb, L. J. *J. Phys. Chem. B* **2015**, *119* (7), 2869−2876.
(16) Walker, D. M.; Wang, R.; Webb, L. J. *Phys. Chem. Chem. Phys.* **2014**, *16* (37), 20047−20060.
(17) Ragain, C. M.; Newberry, R. W.; Ritchie, A. W.; Webb, L. J. *J. Phys. Chem. B* **2012**, *116* (31), 9326−9336.
(18) Schkolnik, G.; Utesch, T.; Salewski, J.; Tenger, K.; Millo, D.; Kranich, A.; Zebger, I.; Schulz, C.; Zimányi, L.; Rákhely, G.; Mroginski, M. A.; Hildebrandt, P. *Chem. Commun.* **2012**, *48* (1), 70.
(19) Schkolnik, G.; Utesch, T.; Zhao, J.; Jiang, S.; Thompson, M. K.; Mroginski, M.-A.; Hildebrandt, P.; Franzen, S. *Biochem. Biophys. Res. Commun.* **2013**, *430* (3), 1011−1015.
(20) Silverman, L. N.; Pitzer, M. E.; Ankomah, P. O.; Boxer, S. G.; Fenlon, E. E. *J. Phys. Chem. B* **2007**, *111* (40), 11611−11613.
(21) Stafford, A. J.; Ensign, D. L.; Webb, L. J. *J. Phys. Chem. B* **2010**, *114* (46), 15331−15344.
(22) Walker, D. M.; Hayes, E. C.; Webb, L. J. *Phys. Chem. Chem. Phys.* **2013**, *15* (29), 12241−12252.
(23) Webb, L. J.; Boxer, S. G. *Biochemistry* **2008**, *47* (6), 1588−1598.
(24) Stafford, A. J.; Walker, D. M.; Webb, L. J. *Biochemistry* **2012**, *51* (13), 2757−2767.
(25) Hu, W.; Webb, L. J. *J. Phys. Chem. Lett.* **2011**, *2* (15), 1925−1930.
(26) Fafarman, A. T.; Sigala, P. A.; Schwans, J. P.; Fenn, T. D.; Herschlag, D.; Boxer, S. G. *Proc. Natl. Acad. Sci. U. S. A.* **2012**, *109* (6), E299−E308.
(27) Chin, J. K.; Jimenez, R.; Romesberg, F. E. *J. Am. Chem. Soc.* **2001**, *123* (10), 2426−2427.
(28) Andrews, S. S.; Boxer, S. G. *J. Phys. Chem. A* **2000**, *104* (51), 11853−11863.
(29) Reimers, J. R.; Hall, L. E. *J. Am. Chem. Soc.* **1999**, *121* (15), 3730−3744.
(30) Aschaffenburg, D. J.; Moog, R. S. *J. Phys. Chem. B* **2009**, *113* (38), 12736−12743.
(31) Getahun, Z.; Huang, C. Y.; Wang, T.; De León, B.; DeGrado, W. F.; Gai, F. *J. Am. Chem. Soc.* **2003**, *125* (2), 405−411.
(32) Bagchi, S.; Fried, S. D.; Boxer, S. G. *J. Am. Chem. Soc.* **2012**, *134*, 10373−10376.
(33) Choi, J.-H.; Oh, K.-I.; Lee, H.; Lee, C.; Cho, M. *J. Chem. Phys.* **2008**, *128* (13), 134506.
(34) Ritchie, A. W.; Webb, L. J. *J. Phys. Chem. B* **2014**, *118* (28), 7692−7702.
(35) Adhikary, R.; Zimmermann, J.; Dawson, P. E.; Romesberg, F. E. *ChemPhysChem* **2014**, *15*, 849−853.
(36) Ritchie, A. W.; Webb, L. J. *J. Phys. Chem. B* **2015**, *119* (44), 13945−13957.
(37) Fafarman, A. T.; Sigala, P. A.; Herschlag, D.; Boxer, S. G. *J. Am. Chem. Soc.* **2010**, *132* (37), 12811−12813.
(38) Zhang, W.; Markiewicz, B. N.; Doerksen, R. S.; Smith, A. B., III; Gai, F. *Phys. Chem. Chem. Phys.* **2016**, *18* (10), 7027−7034.
(39) Ormö, M.; Cubitt, A. B.; Kallio, K.; Gross, L. a; Tsien, R. Y.; Remington, S. J. *Science* **1996**, *273* (5280), 1392−1395.
(40) Chalfie, M.; Tu, Y.; Euskirchen, G.; Ward, W. W.; Prasher, D. C. *Science* **1994**, *263* (5148), 802−805.
(41) Niwa, H.; Inouye, S.; Hirano, T.; Matsuno, T.; Kojima, S.; Kubota, M.; Ohashi, M.; Tsuji, F. I. *Proc. Natl. Acad. Sci. U. S. A.* **1996**, *93* (24), 13617−13622.
(42) Chattoraj, M.; King, B. a; Bublitz, G. U.; Boxer, S. G. *Proc. Natl. Acad. Sci. U. S. A.* **1996**, *93* (16), 8362−8367.
(43) Tsien, R. Y. *Annu. Rev. Biochem.* **1998**, *67*, 509−544.
(44) Ai, H. W.; Shaner, N. C.; Cheng, Z.; Tsien, R. Y.; Campbell, R. E. *Biochemistry* **2007**, *46* (20), 5904−5910.
(45) Wachter, R. M.; Elsliger, M. A.; Kallio, K.; Hanson, G. T.; Remington, S. J. *Structure* **1998**, *6* (10), 1267−1277.

DOI: 10.1021/jacs.6b02156
J. Am. Chem. Soc. 2016, 138, 6561−6570

(46) Shaner, N. C.; Patterson, G. H.; Davidson, M. W. *J. Cell Sci.* **2007**, *120* (24), 4247−4260.
(47) Bublitz, G.; King, B. A.; Boxer, S. G. *J. Am. Chem. Soc.* **1998**, *120* (36), 9370−9371.
(48) Pédelacq, J.-D.; Cabantous, S.; Tran, T.; Terwilliger, T. C.; Waldo, G. S. *Nat. Biotechnol.* **2006**, *24* (1), 79−88.
(49) Schultz, K. C.; Supekova, L.; Ryu, Y.; Xie, J.; Perera, R.; Schultz, P. G. *J. Am. Chem. Soc.* **2006**, *128* (43), 13984−13985.
(50) Liu, C. C.; Schultz, P. G. *Annu. Rev. Biochem.* **2010**, *79* (1), 413−444.
(51) Miyake-Stoner, S. J.; Refakis, C. A.; Hammill, J. T.; Lusic, H.; Hazen, J. L.; Deiters, A.; Mehl, R. A. *Biochemistry* **2010**, *49* (8), 1667−1677.
(52) Hammill, J. T.; Miyake-Stoner, S.; Hazen, J. L.; Jackson, J. C.; Mehl, R. A. *Nat. Protoc.* **2007**, *2* (10), 2601−2607.
(53) Dippel, A. B.; Olenginski, G. M.; Maurici, N.; Liskov, M. T.; Brewer, S. H.; Phillips-Piro, C. M. *Acta Crystallogr. Sect. D Struct. Biol.* **2016**, *72* (1), 1−10.
(54) Rosell, F. I.; Boxer, S. G. *Biochemistry* **2003**, *42* (1), 177−183.
(55) Fafarman, A. T.; Boxer, S. G. *J. Phys. Chem. B* **2010**, *114* (42), 13536−13544.
(56) Henderson, J. N.; Gepshtein, R.; Heenan, J. R.; Kallio, K.; Huppert, D.; Remington, S. J. *J. Am. Chem. Soc.* **2009**, *131* (12), 4176−4177.
(57) Ritchie, A. W.; Webb, L. J. *J. Phys. Chem. B* **2013**, *117* (39), 11473−11489.
(58) Purcell, K. F.; Drago, R. S. *J. Am. Chem. Soc.* **1966**, *88* (5), 919−924.
(59) Fawcett, W. R.; Liu, G.; Kessler, T. E. *J. Phys. Chem.* **1993**, *97*, 9293−9298.
(60) Zimmermann, J.; Thielges, M. C.; Seo, Y. J.; Dawson, P. E.; Romesberg, F. E. *Angew. Chem., Int. Ed.* **2011**, *50*, 8333−8337.
(61) Adhikary, R.; Zimmermann, J.; Dawson, P. E.; Romesberg, F. E. *Anal. Chem.* **2015**, *87* (22), 11561−11567.

DOI: 10.1021/jacs.6b02156
J. Am. Chem. Soc. 2016, 138, 6561−6570